Under Pressure Identification and Characterization: An Upper Cretaceous Belly River Group CO_2 Storage Complex Example

Osadetz K.G.[1], Utting, N.[2], Behmanesh, H.[1], Muravieva, S.[3], Macquet, M.[1], Werner, T.[3] and Lawton, D.C.[1,4]

[1]*Carbon Management Canada, T2L 2K8 Canada.*
[2]*Natural Resources Canada – CanmetENERGY, T9G 1A8 Canada.*
[3]*Axial Insight Ltd., T2W 2R4 Canada.*
[4]*Department of Earth, Energy and Environment, University of Calgary, T2N 1N4 Canada.*

SUMMARY

Upper Cretaceous Belly River Gp. CO_2 storage complex pore pressure, as a function of depth and time, is described by water level monitoring, subsurface gauges and water column pressure loggers. Observations at a deep (~350 m) observation well completed in the CO_2 injection zone (291-298 mbgs) imply an original injection zone pore pressure of ~2.44 MPa. Data from six water wells (<110 m deep) define both, the top of the under pressured zone (51 mbgs) and the head profile that begins at ~53 m depth. The water well head profile extrapolated to the injection zone depth indicates an original injection zone pore pressure of ~2.45 MPa. On May 16th, 2022 an engineering intervention reduced the water column in the deep observation well. Gauge pressure then increased until April 4th, 2023 when it reached 1.83 MPa. Subsequently the gauge pressure has not changed significantly to January 29th, 2024. The regional water table is ~13m deep. At the deep observation well the inferred original injection zone pressure is ~0.5 MPa lower than a freshwater column to surface, but ~1.0 MPa higher than injection zone pressures inferred only 30 m away and >0.60 MPa higher than the observation in the same well after the water level reduction. Since April 2023 the observation well gauge pressure, while much below the originally inferred reservoir pressure, was higher than that inferred in the injection zone after long shut-in periods. The observations are paradoxical considering Boyle's law, such that we conclude the storage complex under pressure, as a function of time, location and depth, consists of two components. The first is an "original" regionally and stratigraphically extensive under pressure. Commonly, in both WCSB and elsewhere, the total under pressure is attributed to either epeirogenesis or glacial loading and unloading, possibly in association with lithospheric flexure. At this location, reservoir paragenesis is inconsistent with the commonly preferred epeirogenic mechanism in favour of a glacial loading and unloading mechanism, possibly with associated lithospheric flexure. We propose that the second under pressure component is "induced" accompanying some engineering interventions. The induced under pressure component is unpredictable spatially and temporally heterogeneous as shown by the deep observation well, and its causes remain problematic. It always additionally reduces the original under pressure, but unpredictably so, often over short distances unlike either the geographic and temporal changes in glacial loads or eroding landscapes, both of which have long spatial wavelengths.

INTRODUCTION

The pore pressure distribution in a well indurated sedimentary succession is commonly close to the hydrostatic pressure as a function of hydrogeological boundary conditions and pore fluid density. Transient pressures occur where additional processes result in either naturally occurring over- or under pressures. Over-pressures commonly fall into two main groups, those related to petroleum phases in reservoirs, which provides reservoir energy for petroleum production, or compaction disequilibrium resulting from an inability of pore space water to migrate out of lithologies accompanying rapid burial, diagenesis or compaction of clay-rich rocks or gypsum (Bradley, 1975; Birchall et al. 2002). Naturally occurring under pressures are less common, although a recent review provides a global phenomenological catalogue (Birchall et al., 2022). The compilation indicates that under pressure occurrences, are with a single exception, terrestrial, occur both in porous and imporous lithologies, attributable to several potential mechanisms acting individually or together, and, by their analysis, similar in magnitude and depth. Birchall et al. (2022) note that the maximum under pressure magnitude among global locations is between 0.5 - 15 Mpa, or between 88%-1% of the expected hydrostatic pressure. However, they neither indicate whether the region of the under pressure was glaciated, nor the claimed duration of the under pressure conditions, which ranges from thousands (Wangen et al. 2016) to hundreds of millions of years (Clark et al., 2013, 2015).

Many under pressure occurrences are attributed to a poro-elastic response accompanying unloading of imporous or low permeability lithologies that increases pore volume and reduces pressure. All infer that the total observed under pressure is attributable to a single or combination of natural processes related only to geological history. They commonly appeal to long-wavelength erosional or deglaciation unloading mechanisms. However, an early and common observation was that the pressure variation is unpredictable spatially and often highly variable, even at similar depths, over short distances (Parks and Toth, 1995; Bekele et al.; 2003; Clark et al. 2013; 2015). Neither do any of the studies consider the diagenetic history of the rocks, or whether there are any indications for strain or pore space reduction that would preclude a elastic response of the lithologies accompanying exhumation or deglaciation.

The most common under pressuring mechanism are sedimentation followed by epeirogenic uplift and erosion or glacial loading and unloading (direct loading of Nuezil, 2012; Birchall et al., 2022), possibly augmented by lithospheric flexure, associated with the imposition and removal of stratigraphic or glacial masses (flexural loading of Neuzil, 2012). Osmotic pressure (Neuzil, 2000) and non-wetting gas phases in the presence of single or multiphase pore fluids are also proposed causes of under pressures (Normani et al., 2017). Common arguments about mechanism and timing are, unfortunately, not independent. The variably eroded and exposed continental landmasses are commonly the locations of Pleistocene and Holocene terrestrial icesheets and glaciers, especially in the Northern Hemisphere and Antarctica, but also in mountain ranges, even at low latitudes. The most intense discussion has been in North America, in both the Western Canada Sedimentary Basin and Michigan Basin. At both locations the primary question addressed is the relative importance of epeirogenic unloading versus glacial unloading. Several analyses include model simulations to explain the causes of subsurface under pressure formation and duration. These commonly use a variety of methods of variable complexity to analyze the magnitudes of strain variations with time (e.g. Normani et al., 2017 versus Kahdar and Novakowski, 2014). The various computational models have yet to identify diagnostic observables that would improve the understanding of the mechanism(s) (e.g. compare Normani et al., 2017 and Kahdar and Novakowski, 2014).

In contrast, observations and arguments presented below suggest that observational paradoxes indicate that part of the observed under pressure is not the result of historical processes, but that it can be induced by engineering interventions and processes yet to be established. We also suggest that the consideration of other data, like diagenetic strain reduction may contribute to the future analysis and possible resolution of the causal and mechanistic problems of under pressure formation and persistence.

STRATIGRAPHIC SETTING

The storage complex is accessed through an injection well 100-10-22-017-16W4 (-112.120°; 50.450°) at Carbon Management Canada's Newell County Facility, also known as the CaMI Field Research Station (Lawton et al., 2019; Macquet et al., 2022). The storage complex comprises Campanian Belly River Group, predominantly sandstone with lesser coal, siltstone and shale (Dawson, 1883; Russell and Landes, 1940; Crockford, 1949). In ascending order, Belly River Gp. consists of Foremost, Oldman and Dinosaur Park formations, all of which are recognized. Foremost Fm. Belly River Group (Glombick, 2010) conformably and gradationally overlies Pakowki Fm, predominantly marine shale. Hamblin and Abrahamson (1996) described the transition from Pakowki shales to Foremost sandstones as a shelf to shoreface transition marked by eastward pro-grading basal sandstone bodies that accompanied west to east progradation of an Upper Cretaceous clastic wedge derived from the Cordilleran orogen. Foremost Fm., commonly shallow marine to paludal sandstones, contains the MacKay and Taber coal zones. Foremost Fm. is conformably overlain by Oldman Fm. (restricted), predominantly fluvial facies, that is itself disconformably overlain by Dinosaur Park Fm. that contains the Lethbridge coal zone at its top. The Oldman Formation was restricted to comprise only a lower predominantly fluvial succession, that is unconformably onlapped by Dinosaur Park Fm., predominantly estuarine sandstones, and a harbinger of the Bearpaw sea transgression and the deposition of marine shale during late Campanian time (Eberth and Hamblin, 1993; Hamblin, 1997). The storage complex is located at the eastern erosional limit of Bearpaw Shale. Basal Belly River shoreface sandstones comprise the storage complex injection zone (Lawton et al., 2019; Macquet et al., 2022). Specifics of the Injection zone reservoir petrology and diagenesis are discussed by Muravieva et al. (2017).

PREVIOUS WORK

Three AER regulated deep wells are operated by CMC at the site. These included the above-mentioned injector (T.D. 545 mbgs) and two variously completed observation wells, both T.D. 344 mbgs, only one of which (101-10-22-016-17W4) is completed through a sand packed annulus and screened casing intervals in the injection zone. Initial attempts to characterize the storage complex pore pressure profile, especially in the basal sandstone injection zone (290-297 mbgs) used a Modular Formation Dynamics Tester (MDT) wireline tool unsuccessfully. No result attributable to the formation was obtained, possibly due to low formation horizontal permeability.

In general, the horizontal sandstone permeability in Belly River Gp. highly variable, but generally an order of magnitude lower than that commonly expected for similarly porous sandstones in other settings (Vocke et al., 2016). Low injection zone horizontal permeability was subsequently confirmed by routine and special core analysis. Vocke (2016) and Vocke et al. (2016) reported 0.0024 mD < k < 5.7 mD. Raad et al., (2021; 2022) and Yu et al. (2020) modelled aspects of reservoir performance using k_{mean} = 0.1-1.5 mD. Core data was also used to calibrate wireline well log data and Dongas (2016) summarized the injection zone reservoir characteristics as 11% effective porosity and 0.57 mD intrinsic permeability. Raad et al. (2021; 2022) employed a kv/kh permeability anisotropy of 0.1. However this value may be smaller as indicated by cutting gas profile data collected during well construction at the site. An upward $\delta^{13}C_{CH4}$ isotopic depletion trend (Mayer et al., 2015) was observed in methane. A similar upward depletion trend was also observed later in co-eval shales to the east and attributed to an upward diffusional isotopic fractionation (Hendry et al., 2016, 2017).

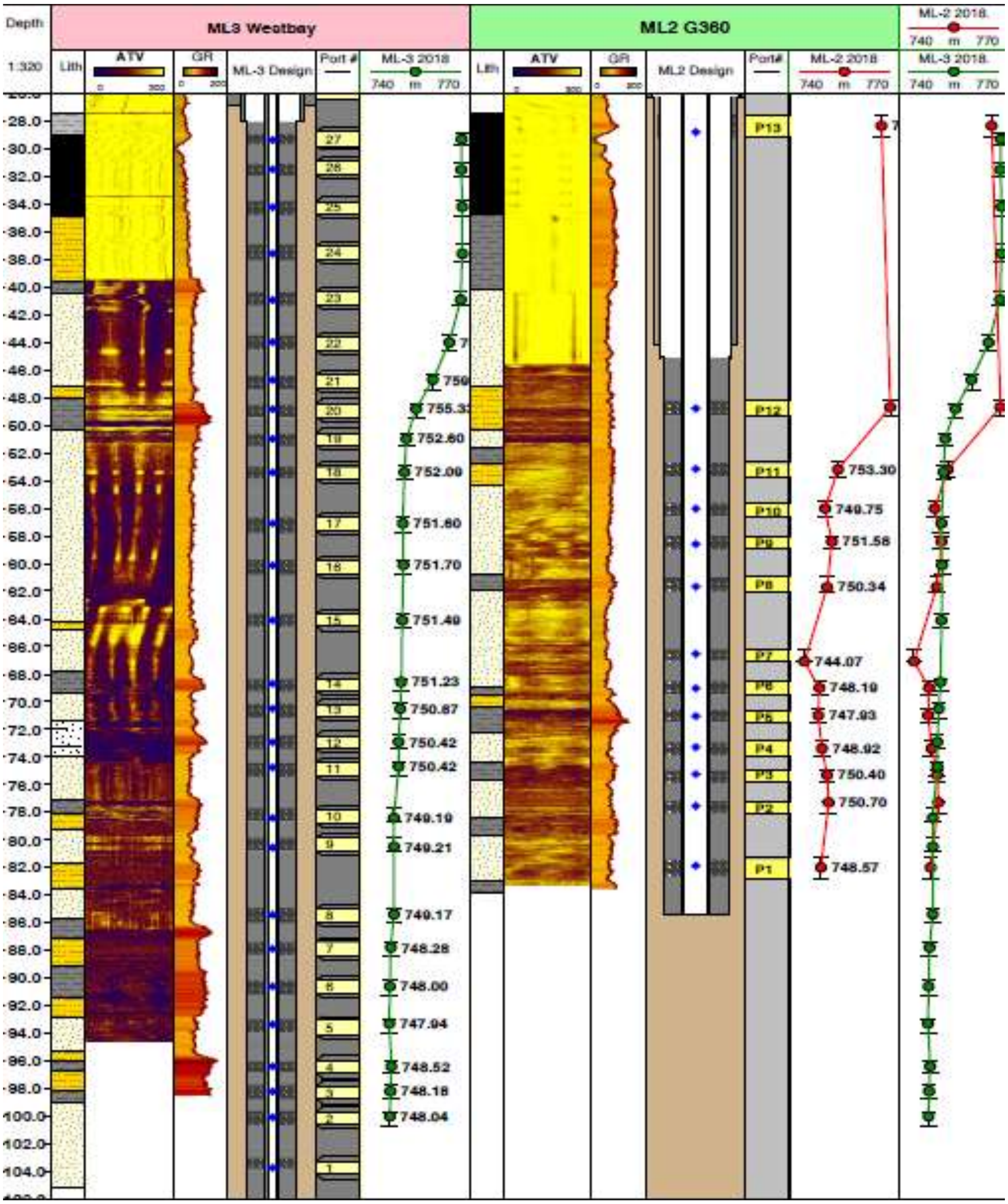

Figure 1. 2018 equilibrated head profiles from ML-3 (Westbay completion, green) and ML-2 (G360 completion, red) from Cheung (2019, Figure A.1).

The shallower hydrogeological environment is well characterized by seven water wells constructed in association with the CO_2 injection program, Two wells have multilevel completions. Another well was cored but was junked prior to completion and abandoned. The site and its vicinity host other water, coal exploration and petroleum wells (Rush, 2016). Local shallow water tables (e.g. +772 m, 7.6 mbgs) in glacial till (Rush, 2016; Cheung, 2019) are likely perched. They depart from the consistent, repeated head profile head measurements in Multi-level (ML) well #3 (ML-3 port 27: head elevation = +768 m, water level ~13 metres below ground surface (bgs)), and in ML-2, DW, and the "2018 shallow" well (slots between +768-767.1m, depth to water ~13-12.5 mbgs) all these wells are completed in Lethbridge coal zone, the shallowest bedrock strata, which also provides the shallowest regional aquifer.

Above 40.9 mbgs (ML-3, port #23) the depth to groundwater at the site follows a freshwater gradient. Cheung (2019) found deeper aquifers exhibited a progressive increase in the depth to groundwater. Depth to groundwater increases rapidly between ML-3 ports 23-20, that are located 40.9-48.8 mbgs. A similar increase in the depth to groundwater occurs between the shallow 2018 water well, compared to the intermediate depth 2018 water well where water levels are ~29 mbgs and the slots are 62.48-63.63 mbgs, as well as at the deep 2018 water well where water levels are ~32 mbgs and the slots are 101.42-104.85 mbgs. In ports below 48.8 mbgs the ML-3 head profile is observed to decrease linearly with increasing depth to the base of the water wells ~100 mbgs. The deeper water levels measured at ML-3 ports are consistent with water levels in the intermediate and deep 2018 water wells, and similar depth intervals of ML-2. Water levels for all aquifers below 53.4m in all wells are under pressured compared to the head profile measured for all aquifers above 40.9 mbgs. Cheung (2019) did not recognize or analyze this under pressured zone nor comment on its significance.

Observation well #1 is equipped with two gauges outside the deeper casing at 286.08 mbgs (290.30 mKB) and 291.68 mbgs (295.80 mKB). The upper gauge is inferred isolated from the formation by impermeable cement and discussed no more. The lower gauge is located within the sand packed annulus between the injection zone and screens in the well casing. Changes in water levels between the injection zone and the casing interior in response to engineering interventions demonstrates communication between the well and the injection zone bedrock. In this well there is agreement among the gauge in the sand pack, and water levels in the well determined by measured well water levels and pressure loggers. The injector is completed with two tubing gauges at 257 mbgs (262.83 mKB) and 267 mbs (272.14 mKB) above the retrievable bridge plug that isolates injection zone perforations from the well casing interior, but which is in communication with the interior of the tubing and the gauges.

STORAGE COMPLEX PORE PRESSURE DATA

Two water wells with different multi-level completions were constructed at the site. These are two examples of similar systems (Kock and Pearson, 2007). ML-3 is located nearest the CO_2 injector and the two deep observations wells. ML-3 is completed with a Westbay system (Westbay Instruments Multilevel Groundwater Monitoring System) of 26 ports between 100 mbgs and 29.3 mbgs. ML-2 is located near the domestic well several hundreds of meters to the south of the CO_2 injector. ML-2 is completed with a less versatile but less expensive Morwick G360 Groundwater Research Institute system (Morwick G360 Groundwater Research Institute (g360group.org)).The multilevel systems permit measurement of hydrogeological parameters, primarily head/aquifer pressure and collection of samples from individual aquifers.

Cheung (2019) compared the 2018 equilibrated head profiles in ML-3 (Figure 1. Westbay, green) and ML-2 (Figure 1, red). In the water wells a normally pressured regime that is consistent with the hydrogeology of jointed bedrock and till that is observed (Grisak et al., 1975; 1976). The transition between the naturally normal pressured and the under pressured parts of the storage complex occurs between 44 mbgs (Port 22, ML-3) and 51 mbgs (Port 19 ML-3) The top of the under pressure is inferred to lie below the depth of post-glacial joints (Hobbs, 1967; Barton, 1972), which are observed in nearby outcrops of Till and Dinosaur Park Fm., along Bow and Red Deer rivers. At Dinosaur Provincial Park some of the till bedrock joints are filled with gypsum or selenite, possibly formed post-glacially. We infer that maximum depth of surface joints will vary, as was observed at the Underground Research Laboratory near Pinawa Manitoba (Everitt and Lajtai, 2004; Everitt, 2018). Although generally similar, the ML-2 data set lacks detail through the transition zone between the shallower, normally pressured, and deeper, under pressured, intervals. We experienced issues obtaining both water level measurements and samples in ML-2. Water level histories in three additional water wells drilled near ML-3, each with single conventional slotted completion over a subset of the same intervals covered by ML-3 are redundant with ML-3 data. Subsequent discussion uses only 2018 equilibrated head data profile from ML-3.

STORAGE COMPLEX PORE PRESSURE ANALYSIS

The ground surface elevation is 779.6 m and the head in the shallowest bedrock aquifers is 766.6 m. In ML-3 port 19 and lower exhibit a very clear linear decline in head with increasing depth that defines the top of the under pressured zone at 51 mbgs (Figure 1). The best-fit slope for the head profile for ports 18 to 2 in the under pressured zone is -9.8×10^{-2} +/- 5.557×10^{-3}. The under pressured head extrapolated to ground surface is 757.4 +/-4.390×10^{-1}, $R^2 = 0.943$, which is 9.2 m deeper than the head in the top of the normally pressured zone. If we extrapolate the under pressured zone head profile in ML-3 ports 18 to 2 to the injection zone we obtain a mean injection zone head elevation of +729.12 m, or an injection zone pore pressure of 2.45 MPa (ρ_{water} = 1020 kg/m^3).

We can also infer injection zone pore pressure independently using a variety of consistent data observations from observation well #1, 30 m away from the injector. Relatively shortly after the completion of observation well #1 the well was subject to significant engineering interventions. This included an N_2 lift that removed the water column in early March 2017 to facilitate a geophysical experiment. That action induced a short period of low-rate gas production in the well. A weighted water column was introduced to suppress the gas flow into the well in mid-September 2017. Downhole gauge data at observation well #1 were recorded after mid-June 2018 and the first water level measurement was made in early July 2018. A pressure logger was introduced early March 2020 and removed in late April 2022 (Figure 2). The physical water level and pressure logger measurements confirmed the function and calibration of the observation well lower gauge in the sand pack. Since late April 2022 the water column measurement is inferred from the lower gauge data after accumulated head space gas pressure is exhausted.

The water column in this well is disturbed slightly by episodic U-Tube sampling ten times between mid-June 2018 and December 2023. U-tube sampling effects are minor compared to the natural reduction in hydrostatic head over time, particularly after the installation of the pressure logger, the restrictions of site access during the COVID-19 work restrictions, and the reduction of U-tube sampling events. The natural reduction of head after the installation of the pressure logger indicates water flow from the well into the injection zone driven by the pressure difference between the injection zone pore pressure and the introduced weighted water column pressure. A dropping water level implies mass transfer and pressure communication among the casing water column, the sand pack, and the injection zone. The measured water levels the injection zone pore pressure is inferred to be, 2.44 MPa (Figure 3). This result from a well located 30 m northeast of the injector is consistent with all the water well data, especially the head profile in ML-3 at that is located 70 m southeast of the injector, that indicated and injection zone pore pressure of 2.45 MPa.

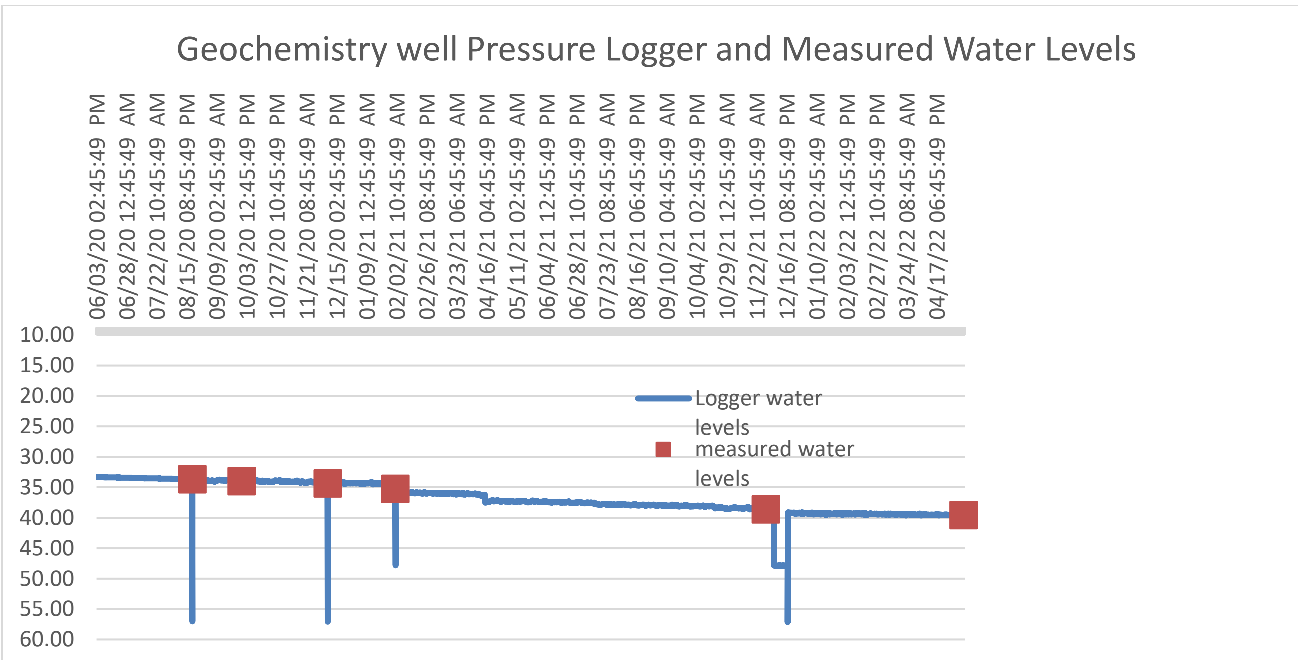

Figure 2. Reduction in observation well #1 head, shown as a depth from ground surface to the top of the water column during the period when the pressure logger (blue line) was recording between June 3rd, 2020, and April 30th, 2022. Orange boxes are direct water level measurements during a similar interval.

A subsequent engineering intervention lowered the water level in observation well #1 to ~150 mbgs on May 16th, 2022. Mass transfer and pressure communication between the interior of observation well #1 and the injection zone was confirmed by the progressive increase in gauge pressure after the 2022 swabbing event. Gauge pressure increased until April 4th, 2023 when it reached 1.83 MPa. Subsequently the observation well lower gauge pressure has not changed significantly to January 29th, 2024.

Injection well gauge pressure transients were observed between November 21st, 2017 and January 16th, 2023 during a dozen extended shut-in intervals, lasting individually between 85 and 30 days. These too are analyzed to infer injection zone pore pressures. The longest shut-in event began July 17, 2018 following the cumulative injection of 7.8 tonnes of CO_2. Within 20 days the gauge pressures approached 1.5 MPa and during the interval between 60 and 85 days the shallower and deeper gauge pressures were essentially constant and respectively 1480.94 kPa and 1484.30 kPa. The pressure gradient between the two gauges during this last interval was also a constant 0.338 kPa/m, indicating a gas phase between the two gauges that can be reasonably inferred to extend into the storage complex. The distance from the lower gauge to the middle of the perforated interval is 26.24 m. From this we infer an injection zone pore pressure at the perforation mid-point ~1493 kPa, if CO_2 density variations with depth are neglected.

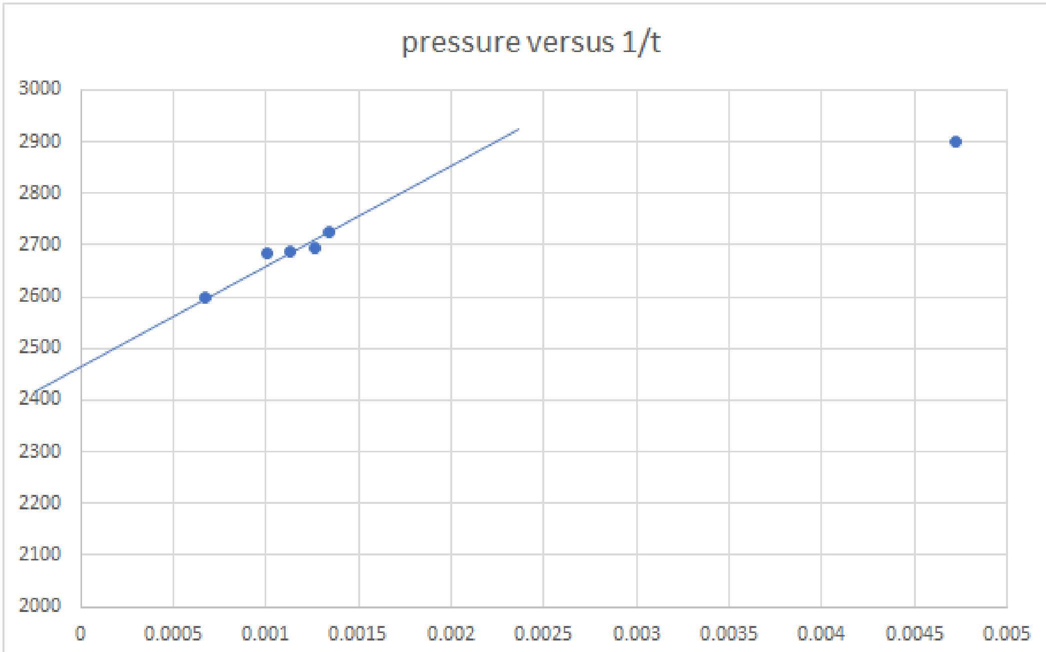

Figure 3. Inference of injection zone initial aquifer pressure from measured water levels in observation well #1. The inferred initial injection zone pressure is 2.44 MPa, which is similar to the result obtained by the downward extrapolation of the ML-3 head profile.

To summarize, water level data from water wells and observation well #1 indicated the storage complex was originally under pressured below 51 mbgs. The water filled injection zone initial pore pressure was inferred to be ~2.44 MPa even after complex engineering interventions and a short period of low-rate gas production followed by the introduction of a weighted water column that suppressed gas flow into the well. Injection zone pore pressure at the injector was not established prior to CO_2 injection. However, early in the CO_2 injection program the injection zone pore pressure data was ~1493 Kpa, or about 60% of the water-filled pore pressure determined only 30 metres away. The anomalously low pore pressures at the end of long shut-in periods persisted until at least early August 2020. A later engineering intervention at the observation well in mid-May 2022 reduced the water column to 150 mbgs. Subsequently the head elevation rose in that well to 1.83 MPa on April 4th, 2023, and this has not changed significantly to January 29th, 2024.

Together these observations indicate that a continuous under pressure in the storage complex extends from 51 mbgs to the base of the CO_2 injection zone or lower. Engineering interventions including hydrostatic head changes and CO_2 injection are temporally associated with augmentation of the under pressure in an unpredictable and non-systematic manner, even over short distances, on time scales varying from months to years. However other engineering interventions at the observation well, including both earlier manipulations of the head and natural gas production, on the time scale of days and months did not result in permanent changes of the hydrogeological system as the water column introduced in June 2018 indicated an equilibrium pore pressure of 2.44 MPa, similar consistent with the regional head profile in the under pressured zone.

DISCUSSION

The multilevel water well head data, that describe the top of the under pressured zone are consistent with the inferred injection zone pore pressure inferred at observation well #1, even after the initial intervention which evacuated the observation well water column leading to a short period of low rate natural gas production before that well was refilled to surface. This coherent and consistent data set is inferred to describe the original hydrogeological system, both in and above the under pressured zone. In addition, the under pressured zone is consistent with the observations from the methane carbon isotopic cuttings gas profile (Mayer et al., 2015), and the interpretation elsewhere that mechanism of upward carbon isotopic depletion indicates a diffusional fractionation in system of very low vertical permeability. From this we conclude that the hydrostatic head/pore pressure profile in under pressured zone below 51 mbgs extends continuously to the base of Belly River Gp, including the injection zone sandstones, and lower. All these data imply an injection zone pore pressure of 2.44-2.45 MPa prior to the construction of the wells at the site.

However, we also observe that the injection zone pore pressure at the injector was often inferred to be $\leq$1.5 MPa during protracted shut-in periods between December 2018 and late February 2021. More recently, the injection zone pore pressure in the observation well has not exceeded 1.83 MPa since early April 2023. From this we conclude that injection zone pressures <2.44 MPa in either the injector or observation well #1 are attributable to an additional mechanism, associated with engineering interventions that reduces injection zone pressure below the original water filled pore pressure.

However, these observations are paradoxical, primarily because they appear to violate both Boyle's Law and Newton's First Law simultaneously. If the pressure decreases in the injection zone then the gas phase fluid must occupy a larger volume within the storage complex, assuming that storage complex is isolated from a sink like the atmosphere. This is reliably assured by the fact the gauges on the injection tubing commonly reach pressures exceeding 5.5 MPa during active CO_2 injection. To occupy a larger volume the injected gas must do work against the adjacent pore space fluids, which, assuming that the injected gas phase is continuous, will occur only when the pressure in the reservoir beyond the plume is less than the sum of the pore space fluid pressure and the storage complex capillary pressure. Any mechanism that simply compresses the existing gas in the plume does not provide a solution to this enigma.

One plausible mechanism for reducing the pressure would be for CO_2 to become dissolved in pore space water. Boyle's law would suggest that up to 39% of the injected CO_2 would have to be dissolved in formation water if the pressure reduction was entirely attributable to a dissolution mechanism. It is true that the solubility of CO_2 in formation water is considerable, particularly if the formation and pore water are cooled by a phase change from liquid CO_2 in the well, as has been observed into gaseous CO_2 in the reservoir, during hiati in the injection program, which are common. Ideal equilibrium dissolution indicates that this is possible.

However, we tend to presume that this is an unlikely explanation for the observed under pressures. There are three primary reason for this, both of which are illustrated by the under pressure in Belly River Gp. sandstones at the Pembina oil field.

1. Similar, and sometimes even larger, under pressures are observed in wells, such as in the Belly River Gp. at the Pembina Field, where the gas phase is natural gas. The aqueous solubility of methane is exceedingly low. Most of the under pressure occurrences are associated with producing gas wells rather than with CO2 injection wells, primarily because of the small number of the latter. If we presume that a single under pressure mechanism occurs in WCSB, this makes the dissolution explanation less attractive.

2. If augmented under pressures were primarily attributable to dissolution mechanism, then we would expect to see systematic and predictable variations in the magnitude of the under pressure. However, this is not observed, rather as explained above the magnitude of the augmented under pressure is spatially chaotic and temporally unpredictable, as indicated since May 2022 at observation well #1. For that matter, if the augmented under pressure was attributable to either epeirogenic or glacial unloading and elastic response of the sedimentary rock succession we would expect to find geographic variations in the magnitude of the under pressure at scales comparable to the epeirogenic or glacial loads that were removed. This is clearly not observed.

3. Similarly geophysical monitoring at this site indicates plume characteristics that are consistent with most of the injected CO2 remaining in a gaseous phase (Macquet et al., 2023).

For now, the mechanism that augments the naturally occurring under pressure remains enigmatic and undetermined.

However, work at our site offers useful constraints on the mechanism of the natural under pressure. Neuzil (1993) recognized an under pressure in the Upper Cretaceous Pierre Fm. shales that were deposited overlying Belly River Group and equivalent strata. Similar naturally occurring under pressured successions are now recognized globally (Birchall et al., 2022). WCSB under pressures are initially recognized elsewhere in Alberta Belly River Group strata at the Pembina oil field (Parks and Toth, 1995; Bekele et al., 2003). There, like at other occurrences of natural under pressure, the focus has been on the cause. The various roles of unloading either epeirogenic or glacial are debated. Parks and Toth (1995) preferred an epeirogenic mechanism, while others like Bekele et al., (2003) inferred a glacial contribution.

Both the potential epeirogenic and glacial unloading under pressure mechanisms operate in the Western Canada Sedimentary Basin. At the storage complex location estimates of mid-Eocene and younger epeirogenic eroded succession (Nurkowski, 1984; Osadetz et al., 1992) and the maximum Pleistocene Ice Sheet thickness (Gowan et al., 2016) are roughly comparable, which makes a mechanistic preference difficult.

Two observations at our site are problematic for the epeirogenic model. The first is the diagenetic history at the storage complex (Muravieva et al., 2017). At maximum burial the elastic strain of pore space appears to be partially or completely reduced by diagenetic mineral dissolution/precipitation reactions that reduce burial strain. The most important is the deposition of a pore space rimming and reducing clay cement that reduces rock volume by the dissolution and reprecipitation of volcanic rock clasts in arenaceous beds. Whether any elastic strain remained in the rock matrix following this strain reduction is uncertain. Similarly, the final diagenetic phase, a pore filling kaolinite suggests the influence of meteoric waters. If sufficient permeability existed to permit mid-Eocene and later meteoric water infiltration, we must question if the protracted preservation of a natural under pressure could be preserved to the Present. Such mechanistic issues have been similarly debated elsewhere, for example, on the eastern flank of Michigan Basin where some (Clark et al., 2013; 2015) propose that natural under pressures have persisted since Paleozoic time. In fact, Normani et al. (2017) who did not distinguish natural from augmented under pressure components in a model study on the eastern flank of Williston Basin favoured, "a state where under pressured conditions predate the onset of glaciation and are better able to preserve the present day helium tracer profile in 260 Ma exhumation analysis".

We have yet to model the natural under pressure component defined by multiple consistent hydrogeological observations at our site, but together with the diagenetic constraints that require the isolation under pressured zone from the epeirogenic groundwater regime after the precipitation of the final pore filling kaolinite mineralization, we lean toward a glacial mechanism as the cause of the naturally occurring under pressure component.

Important implications, with a significance beyond our CO_2 storage pilot, attend these observations. We infer hydrogeological continuity within the naturally under pressured zone that characterizes 87% of the thickness of the Belly River storage complex. Only the uppermost Dinosaur Park Fm., at depths less than 44 mbgs (Port 22, ML-3) the hydrogeological system is inferred normally pressured, especially where surface jointing is present. Since the depth of surface joints varies it could possibly explain why ML-2 heads do not conform better to the consistent pore pressure profile observed at all of ML-3, the three 2018 water wells and observation well #1. The gauge data in both the injector (Behmanesh et. al., 2023) and observation well #1 are both robust and generally well calibrated, even if they indicate conflicting equilibritum storage complex pore pressures.

CONCLUSIONS

1. Deeper water wells indicate and characterize a naturally under pressured zone that begins below 51 mbgs. Within the under pressured zone head profiles decrease linearly with increasing depth. When extrapolated to the injection zone in basal Belly River sandstones water well data suggest an initial injection zone pore pressures of 2.45 MPa.

2. In observation well #1 measured water levels, pressure loggers in the water column and gauge data from the sand pack between the casing and the injection zone are consistent and that all, until May 2022, indicated initial injection zone pressure of 2.44 MPa.

3. We infer that this agreement among multiple independent data sources indicates that initial injection zone regional pore pressure is 2.44-2.45 MPa. Lower injection zone pore pressures at the injection well, inferred from long shut intervals are associated with

engineering interventions that suggest that the natural under pressure can be augmented in response to engineering interventions in the injection zone.

4. The result is paradoxical compared to gauge pressure observations in the injector in consideration of a static gradient test that confirmed the calibration of injector gauges that was performed in April 2022 (Behmanesh, 2023).

5. Currently, we prefer glacial loading and unloading as the cause of naturally occurring under pressure in the storage complex when the diagenetic history of the injection zone is considered.

6. Studies of other under pressured environments should be designed recognizing that engineering interventions may additionally augment the under pressure in ways that remain unexplained.

REFERENCES

Barton, Nick. (1972). A model study of rock-joint deformation. International Journal of Rock Mechanics and Mining Sciences & Geomechanics Abstracts. 9. 579-582. 10.1016/0148-9062(72)90010-1.

Behmanesh, Hamid, Cooper, Joanna, Macquet, Marie, Kolkman-Quinn, Brendan, Lawton, Donald, Osadetz, Kirk, and Greg Maidment. 2023 "Static Gradient Survey Reveals Temperature Anomaly in the CaMI CO_2 Injection Well." Paper presented at the SPE Canadian Energy Technology Conference and Exhibition, Calgary, Alberta, Canada, March 2023. doi: https://doi.org/10.2118/212813-MS

Bekele, E.B., Rostron, B.J., and Nadon, G.C., 2003. Fluid pressure implications of erosional unloading, basin hydrodynamics and glaciation in the Alberta Basin Western Canada. Journal of Geochemical Exploration, 78, p. 143-147. https://doi.org/ 10.1016/S0375-6742(03)—1.

Birchall, T., Senger, K., Swarbrick R. (2022); Naturally occurring underpressure – a global review. *Petroleum Geoscience.* 28 (2): 2021–051. doi: https://doi.org/10.1144/petgeo2021-051

Bradley, J.S. 1975. Abnormal Formation Pressure. *AAPG Bulletin.* 59(6): 957–973. doi: https://doi.org/10.1306/83D91EFC-16C7-11D7-8645000102C1865D

Cheung, T. T. (2019). Establishing High-Resolution Hydrogeological, Geochemical and Isotopic Baseline Conditions of the Fresh Water Zone at a Field Research Site Near Brooks, Alberta, Canada (Unpublished master's thesis). University of Calgary, Calgary, AB. http://hdl.handle.net/1880/111381.

Clark, I.D., Jensen, T. Al, Kennell, M., L., Mazurek, M., Mohapatra, R., Raven; K.G., 2013. Paleozoic-aged brine and authigenic helium preserved in an Ordovician shale aquiclude. Geology, 41 (9): 951–954. doi: https://doi.org/10.1130/G34372.1

Clark, I.D., Ilin, D., Jackson, R.E., Jensen, M., Kennell, L., Mohammadzadeh, H., Poulain, A., Xing, Y.P., Raven, K.G., 2015. Paleozoic-aged microbial methane in an Ordovician shale and carbonate aquiclude of the Michigan Basin, southwestern Ontario. Org. Geochem. 83e84, 118e126. https://doi.org/10.1016/ j.orggeochem.2015.03.006.

Crockford M. B. B. (1949) Oldman and Foremost Formations of Southern Alberta. *AAPG Bulletin*; 33(4): 500–510. doi: https://doi.org/10.1306/3D933D31-16B1-11D7-8645000102C1865D

Dasgupta, T., Mukherjee, S. (2020). Pore Pressure Determination Methods. In: Sediment Compaction and Applications in Petroleum Geoscience. Advances in Oil and Gas Exploration & Production. Springer, Cham. https://doi.org/10.1007/978-3-030-13442-6_3

Dawson, G.M. (1883): Preliminary report on the geology and the Bow and Belly River region, Northwest Territory, with special reference to the coal deposits; Geological Survey of Canada, Report of Progress, 1800–1882, pt. B, p. 1–23.

Dongas, J. M. (2016). Development and Characterization of a Geostatic Model for Monitoring Shallow CO_2 Injection (Unpublished master's thesis). University of Calgary, Calgary, AB. doi:10.11575/PRISM/25635, http://hdl.handle.net/11023/2819

Eberth, D.A. and Hamblin, A.P. (1993): Tectonic, stratigraphic, and sedimentologic significance of a regional discontinuity in the upper Judith River Formation (Belly River wedge) of southern Alberta, Saskatchewan, and northern Montana; Canadian Journal of Earth Sciences, v. 30, p. 174–200.

Everitt, R.A. (2018) Subsurface fracture distribution and its correlation with the shape and thickness of the Lac du Bonnet batholith Bulletin of Engineering Geology and the Environment, 12 p., https://doi.org/10.1007/s10064-018-1385-4

Everitt, R.A., and Lajtai, E.Z. (2004) The influence of rock fabric on excavation damage in theLac du Bonnett granite. International Journal of Rock Mechanics & Mining Sciences. 41:1277–1303.

Gidley, J.L., Holditch, S.A., Nierode, D.E. et al. 1989. An Overview of Hydraulic Fracturing. In Recent Advances in Hydraulic Fracturing, 12. Chap. 1, 1-38. Richardson, Texas: Monograph Series, SPE.

Glombick, P. (2010): Top of the Belly River Group in the Alberta Plains: subsurface stratigraphic picks and modelled surface; Energy Resources Conservation Board, ERCB/AGS Open File 2010-10, 27 p.

Gowan, E.J., Tregoning, P., Purcell, A., Montillet, J.-P., McClusky, S., 2016. A model of the western Laurentide Ice Sheet, using observations of glacial isostatic adjustment, Quaternary Science Reviews, Volume 139, Pages 1-16, https://doi.org/10.1016/j.quascirev.2016.03.003

Grisak, G. E., and J. A. Cherry. 1975. Hydrogeologic characteristics and response of fractured till and clay confining a shallow aquifer. Canadian. Geotechnical Journal. J., 12, pp. 23–43.

Grisak, G. E., J. A. Cherry, J. A. Vonhof, and J. P. Bleumle. 1976. Hydrogeologic and hydrochemical properties of fractured till in the interior plains region. in: R.F. Leggett ed., "Glacial Till", Special Publication, Royal Society of Canada, pp. 304–335.

Hamblin, A.P. (1997): Regional distribution and dispersal of the Dinosaur Park Formation, Belly River Group, surface and subsurface of southern Alberta; Bulletin of Canadian Petroleum Geology, v. 45, p. 377–399.

Hamblin, A.P. and Abrahamson, B.W., 1996, Stratigraphic architecture of "Basal Belly River" cycles, Foremost Formation, Belly River Group, subsurface of southern Alberta and southwestern Saskatchewan: Bulletin of Canadian Petroleum Geology, v.44, p. 654-673.

Hendry, M.J., Barbour, S.L., Schmeling, E.E., Mundle, S.O.C, and Huang, H. (2016), Fate and transport of dissolved methane and ethane in Cretaceous shales of the Williston Basin, Canada, Water Resour. Res., 52, 11p., doi:10.1002/2016WR019047.

Hendry, M.J., Schmeling, E.E., Barbour, S.L., Huang, H. and Mundle, S.O.C, (2017) Fate and Transport of Shale-derived, Biogenic Methane. Scientific Reports,**7**, 4881, 9 p. https://doi.org/10.1038/s41598-017-05103-8.

Hobbs, D. (1967). The Formation of Tension Joints in Sedimentary Rocks: An Explanation. Geological Magazine, 104(6), 550-556. doi:10.1017/S0016756800050226

Khader, O. and Novakowski, K., 2014. Impacts of Pleistocene glacial loading on abnormal pore-water pressure in the eastern Michigan Basin. Geoluids, v. 14, p. 200-220. https://doi.org/10.1111/gfl.12074.

Koch, R.J. and Pearson, S.G., 2007 , Evaluation of Sampling Systems for Multiple Completion Regional Aquifer Wells at Los Alamos National Laboratory, Report LA-UR-07 -4034, Los Alomos National Laboratory, 62 p. 31140.pdf (nm.gov)

Lawton, D. C., Dongas, J., Osadetz, K., Saeedfar, A., & Macquet, M. (2019). Development and analysis of a geostatic model for shallow CO2 injection at the Field Research Station, Southern Alberta, Canada. *Geophysics and Geosequestration. Cambridge University Press, Cambridge*, *280*, 296.

Macquet, M., Lawton, D.C., Saeedfar, A., Osadetz, K.G., 2019. A feasibility study for detection thresholds of CO_2 at shallow depths at the CaMI Field Research Station, Newell County, Alberta, Canada. *Petroleum Geoscience*; 25(4): 509–518. doi: https://doi.org/10.1144/petgeo2018-135

Macquet, M., Lawton, D., Osadetz, K., Maidment, G., Bertram, M., Hall, K., Kolkman-Quinn, B., Monsegny Parra, J., Race, F., Savard, G., Wang, Y., 2022. Overview of Carbon Management Canada's pilot-scale CO2 injection site for developing and testing monitoring technologies for carbon capture and storage, and methane detection. CSEG Recorder 47/1, 27 p.

Mayer, B., Humez, P., Becker, V., Nightingale, M., Ing, J., Kingston, A., Clarkson, C., Cahill, A., Parker, E., Cherry, J., Millot, R., Kloppmann, W., Osadetz, K., Lawton, D. (2015) Prospects and Limitations of Chemical and Isotopic Groundwater Monitoring to Assess the Potential Environmental Impacts of Unconventional Oil and Gas Development, Proc. Earth and Planet. Sci., **13,** p. 320-323.

Michael, K., S. Bachu, B. E. Buschkuehle, K. Haug, and S. Talman, 2009, Comprehensive characterization of a potential site for CO2 geological storage in central Alberta, Canada, in M. Grobe, J. C. Pashin, and R. L. Dodge, eds., Carbon dioxide sequestration in geological media— State of the science: AAPG Studies in Geology 59, p. 227 – 240.

Morad, S., Ketzer, J.M., De Ros, F., 2000. Spatial and temporal distribution of diagenetic alterations in siliciclastic rocks: implications for mass transfer in sedimentary basins. Sedimentology 47, 95–120.

Muravieva, S., Osadetz, K., and Lawton, D. C., 2017, Petrographic assessment of the Upper Cretaceous Foremost Formation prior to CO_2 injection at Field Research Station, Newell County, Alberta; in Perdersen, K., Kuntz,

B., Latos, K., Fraser, A., Geuder, R., and Barclay, J. (eds.) Canadian Society of Petroleum Geologists, 2017 Core Abstract Booklet, Calgary, May 18-19, 2017, p. 27-31.
Neuzil, C.E., 1993. Low fluid pressure within the Pierre Shale: a transient response to erosion. Water Resources Research, 29, 2007-2020, https://doi.org/10.1029/93WR00406.
Neuzil, C.E., 2000. Osmotic generation of "anomalous" fluid pressures in geological environments". Nature, vol. 403, no. 6766, p. 182-184.
Neuzil, C.E., 2012. Hydromechanical effects of continental glaciation on groundwater systems. Geoluids, v. 12, p. 22-37, https://doi.org/10.1111/j.1468-8123.2011.00347.x
Normani, S.D., Sykes, J.F., Jenson, M.R., and Sykes E.A., 2017. Assessing alternative scenarios for the cause of underpressures in the Ordovician sediments along the eastern flank of the Michigan Basin.
Nurkowski, J. R., 1984, Coal quality, coal rank variation and its relation to reconstructed overburden, Upper Cretaceous and Tertiary plains coals, Alberta, Canada: AAPG Bulletin, v. 68, p. 285 – 295.
Osadetz, K.G., Jones, F.W., Majorowicz, J.A., Pearson, D.E., Stasiuk, L.D.,1992. Thermal History of the Cordilleran Foreland Basin in Western Canada: A Review: in, R.W. Macqueen and D.A. Leckie (eds.) Foreland Basins and Fold Belts, Chapter 9, AAPG Memoir 55, p. 259-278.
Parks, K. and Toth, J. (1995). Field evidence for erosion-induced under-pressuring in Upper Cretaceous and Tertiary strata, west central Alberta, Canada. Bulletin of Canadian Petroleum Geology, 43, p. 281-292.
Raad, S.M.J, Lawton, D., Maidment, G., Hassanzadeh, H. (2021) Transient non-isothermal coupled wellbore-reservoir modeling of CO2 injection — Application to CO2 injection tests at the CaMI FRS site, Alberta, Canada, International Journal of Greenhouse Gas Control, v. 111, 103462, https://doi.org/10.1016/j.ijggc.2021.103462.
Raad, S.M.J, Lawton, D., Maidment, G., Hassanzadeh, H. (2022) Sensitivity analysis of operating parameters affecting CO2 wellbore transient flow at the CaMI Field Research Station, Alberta, Canada, International Journal of Greenhouse Gas Control, Volume 114, 103594, https://doi.org/10.1016/j.ijggc.2022.103594.
Rush, L., 2016. Groundwater dynamics of the CMC Research Site near Brooks, Alberta. senior undergraduate independent studies project, Applied Geochemistry Group, Department of Geoscience, University of Calgary. Available from M. Nightingale, mnightin@ucalgary.ca, 79 p. plus oversized figures.
Russell, L.S. and Landes, R.W. (1940): Geology of the southern Alberta Plains; Geological Survey of Canada, Memoir 221, 223 p.
Utley R.E., Martin-Roberts E., Utting N., Johnson G., Györe D., Zurakowska M., Stuart, F.M., Boyce, A.J., Darrah, T.H., Gulliver, P., Haszeldine, RS, Lawton D and Gilfillan, S.M.V. (2023) Multi-Isotope Geochemical Baseline Study of the Carbon Management Canada Research Institutes CCS Field Research Station (Alberta, Canada), Prior to CO2 Injection. Earth Sci. Syst. Soc. 3:10069. doi: 10.3389/esss.2023.10069
Utting, N., Osadetz, K., Darrah, T. H., Brennwald, M. S., Mayer, B., & Lawton, D. (2022). Methods and benefits of measuring non-hydrocarbon gases from surface casing vents. *International Journal of Environmental Science and Technology*. https://doi.org/10.1007/s13762-022-04300-x
Vocke, C., 2016. Application of profile (probe) permeability and mechanical (rebound) hardness tests for characterization of fluid transport and geomechanical properties of selected formations in Western Canada, B.Sc. Thesis supervised by Dr. C. Clarkson, Department of Geoscience (now Department of Earth, Energy and Environment), University of Calgary,
Vocke, C., Clarkson, C.R., Aquino, S., Vahedian, A., Lawton, D.C., Osadetz, K., and Ghanizadeh, A., 2016. Application of profile (probe) permeability and mechanical (rebound) hardness tests for characterization of fluid transport and geomechanical properties of selected formations in western Canada, Geoconvention 2016 abstract archive, 4 p. https://geoconvention.com/wp-content/uploads/abstracts/2016/134_GC2016_Application_of_profile_probe_permeability.pdf last accessed 2024/02/13.
Wangen, M., Souche, A. and Johansen, H., 2016. A model for underpressure development in a glacial valley, an example from Adventdalen, Svalbard. Basin Research. 28/6: 752-769. doi = https://doi.org/10.1111/bre.12130
Yu, X, Ahmadinia, M, Shariatipour, SM, Lawton, D, Osadetz, K & Saeedfar, A 2020, 'Impact of Reservoir Permeability, Permeability Anisotropy and Designed Injection Rate on CO2 Gas Behavior in the Shallow Saline Aquifer at the CaMI Field Research Station, Brooks, Alberta', Natural Resources Research, vol. 29, no. 4, pp. 2735–2752. https://doi.org/10.1007/s11053-019-09604-3 .